Optical rogue waves associated with the negative coherent coupling in an isotropic medium

Wen-Rong Sun, Bo Tian,* Yan Jiang, and Hui-Ling Zhen
State Key Laboratory of Information Photonics and Optical Communications, and School of Science, Beijing University of Posts and Telecommunications, Beijing 100876, China
(Received 15 September 2014; revised manuscript received 3 December 2014; published 13 February 2015)

Optical rogue waves of the coupled nonlinear Schrödinger equations with negative coherent coupling, which describe the propagation of orthogonally polarized optical waves in an isotropic medium, are reported. We construct and discuss a family of the vector rogue-wave solutions, including the bright rogue waves, four-petaled rogue waves, and dark rogue waves. A bright rogue wave without a valley can split up, giving birth to two bright rogue waves, and an eye-shaped rogue wave can split up, giving birth to two dark rogue waves.

DOI: 10.1103/PhysRevE.91.023205 PACS number(s): 05.45.Yv, 42.65.Tg

I. INTRODUCTION

Ocean rogue waves are rare events [1–6]. The height of a rogue wave is two or more times those of the surrounding waves [5,6]. Besides the ocean waves, rogue waves have been reported in nonlinear optics [7,8], plasmas [9], and microwave systems [10]. Optical rogue waves have been observed in an optical system, based on a microstructured optical fiber [11]. Different kinds of laboratory experiments and theoretical approaches have been performed to study the optical rogue waves [7,8,12,13]. In physical systems such as the Bose-Einstein condensates and optical fibers, vector rogue waves have been introduced [14–17]. Indeed, vector rogue-wave solutions of the three-wave resonant interaction equations, coupled Hirota equations, and Manakov systems have been presented [14–17].

Propagation of the two orthogonally polarized pulses in a monomode birefringent fiber can be described by the coupled nonlinear Schrödinger (CNLS) equations, where the nonlinear coupling terms are related to the third-order susceptibility tensor $\chi^{(3)}$ of the fiber [18–20]. In an isotropic medium, $\chi^{(3)}$ has three independent components and the nonlinear polarization parts that account for the nonlinear coupling terms have also been presented [19,20]. Motivated by that, in an isotropic medium, the CNLS equations with negative coherent coupling describing the propagation of orthogonally polarized optical waves can be written as [18–20]

$$iq_{1t} + q_{1xx} + 2(|q_1|^2 + 2|q_2|^2)q_1 - 2q_1^* q_2^2 = 0, \quad (1a)$$

$$iq_{2t} + q_{2xx} + 2(|q_2|^2 + 2|q_1|^2)q_2 - 2q_2^* q_1^2 = 0, \quad (1b)$$

where q_1 and q_2 are the slowly varying envelopes of two interacting optical modes, the variables x and t, respectively, correspond to the normalized distance and retarded time, and the asterisk denotes the complex conjugate. Equations (1) can describe the light propagation in the paraxial approximation [18–20]. The coefficients of the self-phase modulation and the cross-phase modulation are different [18–20]. The last terms of Eqs. (1) are known as the coherent coupling terms [18–20]. Darboux transformation (DT) of Eqs. (1) has been introduced [20], and integrability properties and soliton solutions of Eqs. (1) have been obtained [19]. Degenerate and nondegenerate vector soliton solutions of Eqs. (1) have been derived with the bilinear system [18a]. More on solitons can be seen in Refs. [18b].

In this paper, we will construct a family of the vector rogue-wave solutions of Eqs. (1). For certain special parameter values and seed solutions, we will obtain the bright rogue waves, four-petaled rogue waves (two humps and two valleys), and dark rogue waves. In Sec. II, using the two different seed solutions and DT, we will construct the vector rogue-wave solutions of Eqs. (1), and different types of vector rogue waves will be shown. Section III will be our discussions and Sec. IV will be our conclusions.

II. DIFFERENT TYPES OF VECTOR ROGUE WAVES

The Lax pair of Eqs. (1) is [19,20]

$$\Psi_x = (\lambda U_0 + U_1)\Psi, \quad \Psi_t = (\lambda^2 V_0 + \lambda V_1 + V_2)\Psi, \quad (2)$$

with

$$U_0 = i\begin{pmatrix} -\mathbf{I}_{2\times 2} & \mathbf{O} \\ \mathbf{O} & \mathbf{I}_{2\times 2} \end{pmatrix}, \quad U_1 = \begin{pmatrix} \mathbf{O} & \mathbf{Q} \\ -\mathbf{Q}^\dagger & \mathbf{O} \end{pmatrix},$$
$$\mathbf{Q} = \begin{pmatrix} q_1 & q_2 \\ -q_2 & q_1 \end{pmatrix}, \quad V_0 = 2i\begin{pmatrix} -\mathbf{I}_{2\times 2} & \mathbf{O} \\ \mathbf{O} & \mathbf{I}_{2\times 2} \end{pmatrix},$$
$$V_1 = 2\begin{pmatrix} \mathbf{O} & \mathbf{Q} \\ -\mathbf{Q}^\dagger & \mathbf{O} \end{pmatrix}, \quad V_2 = i\begin{pmatrix} \mathbf{Q}\mathbf{Q}^\dagger & \mathbf{Q}_x \\ \mathbf{Q}_x^\dagger & -\mathbf{Q}^\dagger\mathbf{Q} \end{pmatrix},$$

where $\Psi = \begin{pmatrix} \varphi_1 & \varphi_2 & \varphi_3 & \varphi_4 \\ -\varphi_2 & \varphi_1 & -\varphi_4 & \varphi_3 \end{pmatrix}^T$ (the superscript T signifies the matrix transpose) is the matrix eigenfunction, φ_i ($i = 1,2,3,4$) are the functions of x and t, $\mathbf{I}_{2\times 2}$ is the 2×2 unit matrix, $\mathbf{O}$ is the 2×2 zero matrix, $\dagger$ denotes the conjugate transpose, and λ is the eigenvalue parameter. Assume that $\Psi = \begin{pmatrix} \varphi_1 & \varphi_2 & \varphi_3 & \varphi_4 \\ -\varphi_2 & \varphi_1 & -\varphi_4 & \varphi_3 \end{pmatrix}^T$ is a solution of Lax pair (2) corresponding to λ, and $\begin{pmatrix} -\varphi_3^* & \varphi_4^* & \varphi_1^* & -\varphi_2^* \\ \varphi_4^* & \varphi_3^* & -\varphi_2^* & -\varphi_1^* \end{pmatrix}^T$ is a solution of Lax pair (2) corresponding to λ^*. The DT $(\Psi, \mathbf{Q}) \to (\widetilde{\Psi}, \widetilde{\mathbf{Q}})$ of Lax pair (2) can be given as [20]

$$\widetilde{\Psi} = (\lambda \mathbf{I}_{4\times 4} - S)\Psi, \quad \widetilde{\mathbf{Q}} = \mathbf{Q} - 2iS_{12},$$
$$S = \begin{pmatrix} S_{11} & S_{12} \\ S_{21} & S_{22} \end{pmatrix} = H\Lambda H^{-1},$$

*Corresponding author: tian_bupt@163.com

$$H=\begin{pmatrix}\varphi_1 & -\varphi_2 & -\varphi_3^* & \varphi_4^*\\ \varphi_2 & \varphi_1 & \varphi_4^* & \varphi_3^*\\ \varphi_3 & -\varphi_4 & \varphi_1^* & -\varphi_2^*\\ \varphi_4 & \varphi_3 & -\varphi_2^* & -\varphi_1^*\end{pmatrix},$$

$$\Lambda=\begin{pmatrix}\lambda & 0 & 0 & 0\\ 0 & \lambda & 0 & 0\\ 0 & 0 & \lambda^* & 0\\ 0 & 0 & 0 & \lambda^*\end{pmatrix},$$

where $\widetilde{\Psi}=(\begin{smallmatrix}\widetilde{\varphi}_1 & \widetilde{\varphi}_2 & \widetilde{\varphi}_3 & \widetilde{\varphi}_4\\ -\widetilde{\varphi}_2 & \widetilde{\varphi}_1 & -\widetilde{\varphi}_4 & \widetilde{\varphi}_3\end{smallmatrix})^T$ satisfies Lax pair (2) with the potential function $\widetilde{\mathbf{Q}}$, $\mathbf{I}_{4\times4}$ is the 4×4 unit matrix, and S_{ij} $(i,j=1,2)$ are the 2×2 matrices.

To obtain the vector rogue-wave solutions of Eqs. (1), we derive the seed solutions of Eqs. (1) as

$$q_1=e^{4it},\quad q_2=e^{4it},\quad \mathbf{Q}=\begin{pmatrix}1 & 1\\ -1 & 1\end{pmatrix}e^{4it}. \tag{3}$$

Next, we will derive the vector eigenfunction which makes Lax pair (2) compatible with seed solutions (3). Splitting the four functions φ_1, φ_2, φ_3, and φ_4 into their real and imaginary parts yields

$$\begin{aligned}&\varphi_1=(\varphi_{1R}+i\varphi_{1I})e^{2it},\quad \varphi_2=(\varphi_{2R}+i\varphi_{2I})e^{2it},\\ &\varphi_3=(\varphi_{3R}+i\varphi_{3I})e^{-2it},\quad \varphi_4=(\varphi_{4R}+i\varphi_{4I})e^{-2it},\end{aligned} \tag{4}$$

where φ_{jI} and φ_{jR} $(j=1,2,3,4)$ are the functions of x and t, and the subscripts R and I mean the real and imaginary parts, respectively. Substituting expressions (4) and seed solutions (3) into Lax pair (2), we obtain

$$\begin{aligned}&\lambda=\sqrt{2}i,\quad \varphi_{1R}=-\frac{\sqrt{2}}{2}t,\quad \varphi_{2R}=-\frac{\sqrt{2}}{2}t-t,\quad \varphi_{3R}=-\frac{\sqrt{2}}{2}t,\quad \varphi_{4R}=\frac{\sqrt{2}}{2}t+t,\\ &\varphi_{1I}=\frac{1}{4}x,\quad \varphi_{2I}=\frac{1}{4}x+\frac{1}{4}+\frac{\sqrt{2}}{4}x,\quad \varphi_{3I}=\frac{1}{4}x,\quad \varphi_{4I}=-\frac{1}{4}x+\frac{1}{4}-\frac{\sqrt{2}}{4}x.\end{aligned} \tag{5}$$

Substituting expressions (5) into DT (3), we derive the vector rogue-wave solutions of Eqs. (1) as follows:

$$q_1=-e^{4it}\frac{F_{11}}{G_{11}},\quad q_2=-e^{4it}\frac{D_{11}}{G_{11}}, \tag{6}$$

where

$$\begin{aligned}F_{11}=&-1-2\sqrt{2}-16it-16i\sqrt{2}t-32t^2-768it^3-512i\sqrt{2}t^3\\ &+1536t^4+1024\sqrt{2}t^4-8x^2-8\sqrt{2}x^2-96itx^2-64i\sqrt{2}tx^2+384t^2x^2+256\sqrt{2}t^2x^2+24x^4+16\sqrt{2}x^4,\\ G_{11}=&1+32t^2+32\sqrt{2}t^2+1536t^4+1024\sqrt{2}t^4+8x^2+4\sqrt{2}x^2+384t^2x^2+256\sqrt{2}t^2x^2+24x^4+16\sqrt{2}x^4,\\ D_{11}=&-1-96t^2-64\sqrt{2}t^2-768it^3-512i\sqrt{2}t^3+1536t^4+1024\sqrt{2}t^4\\ &-96itx^2-64i\sqrt{2}tx^2+384t^2x^2+256\sqrt{2}t^2x^2+24x^4+16\sqrt{2}x^4.\end{aligned}$$

In Fig. 1, it can be seen that $|q_1|^2$ and $|q_2|^2$ have different structures. In the q_1 component, a bright rogue wave with an eye-shaped distribution (a hump and two valleys) is shown in Fig. 1(a), while in the q_2 component, a four-petaled rogue wave (two humps and two valleys) is displayed in Fig. 1(b). We note that the center value of the wave with a four-petaled structure is almost equal to that of the background, as seen in Fig. 1(b).

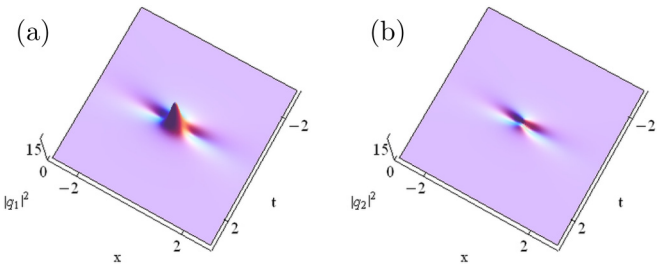

FIG. 1. (Color online) Vector rogue-wave envelope distributions $|q_1|^2$ and $|q_2|^2$ of solutions (6).

The zero seed solution allows one to construct the hierarchy of soliton solutions [20], while plane-wave solutions (3) produce the rational solutions. Hereby, we consider another case in which one is a zero solution and the other is a plane-wave solution, as follows:

$$\begin{aligned}&q_1=0,\quad q_2=e^{2it},\\ &\mathbf{Q}=\begin{pmatrix}0 & 1\\ -1 & 0\end{pmatrix}e^{2it}.\end{aligned} \tag{7}$$

Then, we will find four functions φ_1, φ_2, φ_3, and φ_4 which make Lax pair (2) compatible with seed solutions (7). Substituting seed solutions (7) into Lax pair (2), we obtain

$$\begin{aligned}&\lambda=i,\quad \varphi_1=(x+2it+b)e^{it},\quad \varphi_2=(2x+4it+2)e^{it},\\ &\varphi_3=(2x+4it)e^{-it},\quad \varphi_4=(-x-2it+1-b)e^{-it},\end{aligned} \tag{8}$$

where b is a real parameter.

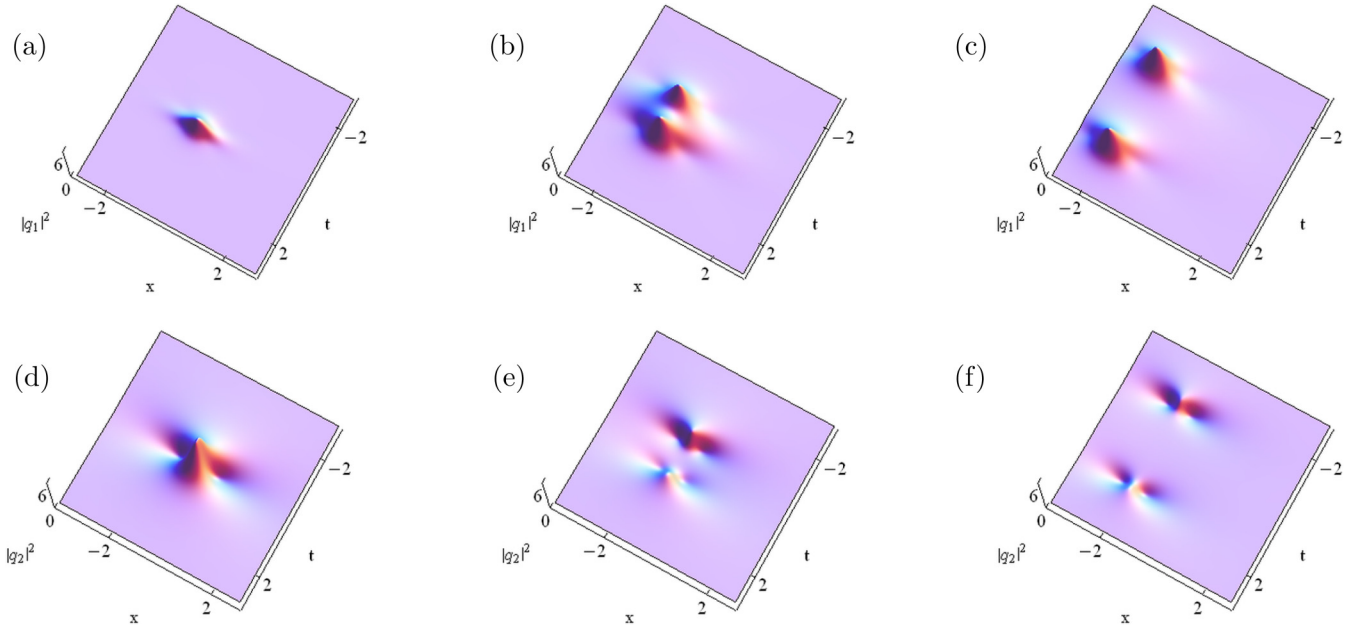

FIG. 2. (Color online) Vector rogue-wave envelope distributions $|q_1|^2$ and $|q_2|^2$ of solutions (9) with (a),(d) $b = 1.5$; (b),(e) $b = 4$; (c),(f) $b = 8$.

Substituting expressions (8) into DT (3), we derive the vector rogue-wave solutions of Eqs. (1) as follows:

$$q_1 = -e^{2it}\frac{F_{12}}{G_{12}}, \quad q_2 = -e^{2it}\frac{D_{12}}{G_{12}}, \tag{9}$$

where

$$\begin{aligned}
F_{12} &= 8(-1+b)(5-2b+2b^2+20it-40t^2+6x+4bx+10x^2),\\
G_{12} &= 25-20b+24b^2-8b^3+4b^4+144t^2+352bt^2-96b^2t^2+1600t^4+60x+16bx+8b^2x+16b^3x\\
&\quad +480t^2x+320bt^2x+136x^2+8bx^2+56b^2x^2+800t^2x^2+120x^3+80bx^3+100x^4,\\
D_{12} &= -25+4b^2-8b^3+4b^4-72it-176ibt+48ib^2t-256t^2+352bt^2-96b^2t^2-1600it^3+1600t^4-24bx\\
&\quad +8b^2x+16b^3x-240itx-160ibtx+480t^2x+320bt^2x+36x^2+8bx^2+56b^2x^2-400itx^2+800t^2x^2\\
&\quad +120x^3+80bx^3+100x^4.
\end{aligned}$$

Figures 2(a)–2(c) show a bright rogue wave without valley splitting in the q_1 component, giving birth to two bright rogue waves. With the decrease of b, the two bright rogue waves merge into the higher-amplitude bright rogue wave, as shown in Fig. 3(a). The distance between the two humps increases with the increase of b, as shown in Figs. 2(b) and 2(c). Figures 2(d)–2(f) show an eye-shaped rogue wave splitting in the q_2 component, giving birth to two dark rogue waves. With the decrease of b, the two dark rogue waves merge into an eye-shaped rogue wave. Different from the phenomenon in Fig. 3(a), the amplitude of the eye-shaped rogue wave decreases with the decrease of b, as shown in Fig. 3(b).

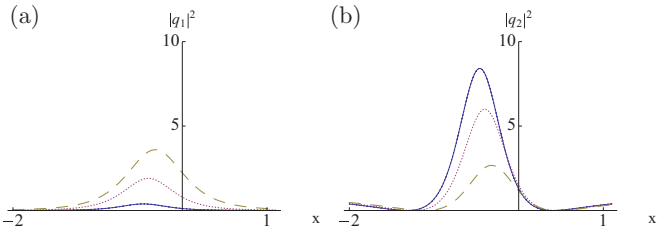

FIG. 3. (Color online) Vector rogue-wave envelope distributions $|q_1|^2$ and $|q_2|^2$ of solutions (9) with $t = 0, b = 0.8$ (solid line), $b = 0.5$ (short dashed line), and $b = 0.1$ (long dashed line).

III. DISCUSSION

(i) For Eqs. (1), attention should be paid to the following aspects: (a) Different from the Manakov system [14,21], the ratio between the coefficients of self-phase modulation and cross-phase modulation is 1:2. (b) Compared with the Manakov system, Eqs. (1) contain the negative coherent coupling. For those reasons, Eqs. (1) admit the different types of vector rogue waves (as shown in Table I), which are different from the Manakov-type vector rogue waves [14,21].

(ii) In Fig. 1, we observe an eye-shaped rogue wave together with a wave with the four-petaled structure. The four-petaled rogue wave in the q_2 component is quite different from the well-known eye-shaped one. Such four-petaled structure

TABLE I. Types of vector rogue waves.

$\|q_1\|^2$	$\|q_2\|^2$
An eye-shaped rogue wave	A wave with the four-petaled structure
A bright rogue wave without valley	An eye-shaped rogue wave
A bright rogue wave with two humps	A dark rogue wave with two humps and four valleys
Two bright rogue waves	Two dark rogue waves

comes from the cross-phase modulation effects since the four-petaled structure cannot be observed in a scalar NLS equation. The possibilities to observe the four-petaled rogue waves of three-wave resonant interaction equations have been discussed [17,22]. Considering a three-wave resonant interaction optical spatial noncollinear scheme with type II second-harmonic generation in a 3-cm-long birefringent KTP crystal [17,23],[1] one can observe the four-petaled rogue waves [17].

(iii) In Fig. 2, we observe a bright rogue wave without the valley splitting in the q_1 component, giving birth to two bright rogue waves, and an eye-shaped rogue wave splitting in the q_2 component, giving birth to two dark rogue waves. Rogue-wave splitting (the behavior in the q_1 component) has been observed in a 3-cm-long birefringent KTP crystal [17]. Reference [17] states, "Spatial diffractionless 6 mm waist beams, mimicking quasi-plane waves, at 1064 nm would lead to the modulational instability evidence." However, the behavior of the rogue wave in the q_2 component has not been reported in the previous studies.

(iv) It is expected that the vector rogue waves [solutions (6) and (9)] could be observed in nonlinear optics. Actually, rogue waves have been experimentally observed in several nonlinear optics systems [11,13]. We briefly discuss the experimental condition for the observation of those vector rogue waves:

(a) One may consider an experiment in a passively mode-locked fiber laser: The laser consists of the two lengths of the single-mode fiber and a 17 cm piece of (single spatial mode) erbium-ytterbium fiber to provide the gain [24,25]. The round-trip cavity is approximately 430 cm in length, which corresponds to a 48 MHz repetition rate [25]. One can see the experimental setup of Refs. [24,25].

(b) Another experimental setup in the mode-locked fiber laser can be seen in Refs. [26,27]. The all-fiber ring laser cavity comprises the dual 980 nm pumping of a 2-m-erbium-doped fiber with the normal dispersion $D = -12.5$ ps nm^{-1} km^{-1} [26]. The highest recorded amplitude here is above 205 mV, while the significant wave height is 63.1 mV. Results show that the pulses can be considered as the rogue waves as their maximal amplitude is 3.2 times that of the significant wave height [26].

[1]Potassium titanium oxide phosphate (KTiOPO4), or KTP, is a nonlinear optical crystal in the visible-to-infrared spectral region with relatively low cost [23].

IV. CONCLUSION

We have analytically constructed and discussed a family of the vector rogue-wave solutions of the CNLS equations with negative coherent coupling, i.e., Eqs. (1), which describe the propagation of orthogonally polarized optical waves in an isotropic medium. Using DT (3), we have derived the vector rogue-wave solutions, i.e., solutions (6) and (9). An eye-shaped rogue wave together with a wave having the four-petaled structure have been shown in Fig. 1. Figures 2(a)–2(c) have displayed a bright rogue wave without valley splitting in the q_1 component, and Figs. 2(d)–2(f), an eye-shaped rogue wave splitting in the q_2 component with the increase of b. The two bright rogue waves have been shown to merge into the higher-amplitude bright rogue wave with the decrease of b, while the two dark rogue waves, to merge into the lower-amplitude eye-shaped rogue wave with the decrease of b, as presented in Fig. 3. It is expected that our results on nonlinear waves could be extended to the periodically driven media [28–31].

Different types of vector rogue waves obtained in this paper have been summarized in Table I.

ACKNOWLEDGMENTS

We express our sincere thanks to the Editors and Reviewers for their valuable comments. This work has been supported by the National Natural Science Foundation of China under Grant No. 11272023, by the Open Fund of State Key Laboratory of Information Photonics and Optical Communications (Beijing University of Posts and Telecommunications) under Grant No. IPOC2013B008, and by the Fundamental Research Funds for the Central Universities of China under Grant No. 2011BUPTYB02.

[1] C. Kharif, E. Pelinovsky, and A. Slunyaev, *Rogue Waves in the Ocean, Observations, Theories and Modeling*, Advances in Geophysical and Environmental Mechanics and Mathematics Series Vol. 14 (Springer, Berlin, 2009).

[2] A. Osborne, *Nonlinear Ocean Waves and the Inverse Scattering Transform* (Elsevier, New York, 2010).

[3] A. Slunyaev, I. Didenkulova, and E. Pelinovsky, Contemp. Phys. **52**, 571 (2011).

[4] N. Akhmediev, J. M. Soto-Crespo, and A. Ankiewicz, Phys. Lett. A **373**, 2137 (2009).

[5] M. Onorato, S. Residori, U. Bortolozzo, A. Montina, and F. T. Arecchi, Phys. Rep. **528**, 47 (2013).

[6] A. Abrashkin and A. Soloviev, Phys. Rev. Lett. **110**, 014501 (2013).

[7] A. Coillet, J. Dudley, G. Genty, L. Larger, and Y. K. Chembo, Phys. Rev. A **89**, 013835 (2014).

[8] C. Liu, Z. Y. Yang, L. C. Zhao, G. G. Xin, and W. L. Yang, Opt. Lett. **39**, 1057 (2014); D. W. Zuo, Y. T. Gao, L. Xue, Y. J. Feng, and Y. H. Sun, Appl. Math. Lett. **40**, 78 (2015); D. W. Zuo, Y. T. Gao, L. Xue, and Y. J. Feng, Chaos, Solitons Fract. **69**, 217 (2014).

[9] H. Bailung, S. K. Sharma, and Y. Nakamura, Phys. Rev. Lett. **107**, 255005 (2011).

[10] R. Höhmann, U. Kuhl, H. J. Stöckmann, L. Kaplan, and E. J. Heller, Phys. Rev. Lett. **104**, 093901 (2010).

[11] D. R. Solli, C. Ropers, P. Koonath, and B. Jalali, Nature (London) **450**, 1054 (2007).

[12] M. Erkintalo, G. Genty, and J. M. Dudley, Opt. Lett. **34**, 2468 (2009).

[13] B. Kibler, J. Fatome, C. Finot, G. Millot, F. Dias, G. Genty, N. Akhmediev, and J. Dudley, Nat. Phys. **6**, 790 (2010).

[14] F. Baronio, A. Degasperis, M. Conforti, and S. Wabnitz, Phys. Rev. Lett. **109**, 044102 (2012).

[15] S. Chen and L. Y. Song, Phys. Rev. E **87**, 032910 (2013).

[16] Y. V. Bludov, V. V. Konotop, and N. Akhmediev, Europhys. J. Spec. Top. **185**, 169 (2010).

[17] F. Baronio, M. Conforti, A. Degasperis, and S. Lombardo, Phys. Rev. Lett. **111**, 114101 (2013).

[18] (a) X. Lü and B. Tian, Phys. Rev. E **85**, 026117 (2012); (b) Y. J. Shen, Y. T. Gao, D. W. Zuo, Y. H. Sun, Y. J. Feng, and L. Xue, *ibid.* **89**, 062915 (2014); Y. J. Shen, Y. T. Gao, X. Yu, G. Q. Meng, and Y. Qin, Appl. Math. Comput. **227**, 502 (2014); Z. Y. Sun, Y. T. Gao, X. Yu, and Y. Liu, Phys. Lett. A **377**, 3283 (2013); Europhys. Lett. **93**, 40004 (2011); Z. Y. Sun, Y. T. Gao, Y. Liu, and X. Yu, Phys. Rev. E **84**, 026606 (2011).

[19] Q.-Han Park and H. J. Shin, Phys. Rev. E **59**, 2373 (1999); **61**, 3093 (2000).

[20] H. Q. Zhang, J. Li, T. Xu, Y. X. Zhang, W. Hu, and B. Tian, Phys. Scr. **76**, 452 (2007).

[21] B. L. Guo and L. M. Ling, Chin. Phys. Lett. **28**, 110202 (2011).

[22] L. C. Zhao and J. Liu, Phys. Rev. E **87**, 013201 (2013).

[23] F. Baronio, M. Conforti, C. De Angelis, A. Degasperis, M. Andreana, V. Couderc, and A. Barthélémy, Phys. Rev. Lett. **104**, 113902 (2010).

[24] S. T. Cundiff, B. C. Collings, N. N. Akhmediev, J. M. Soto-Crespo, K. Bergman, and W. H. Knox, Phys. Rev. Lett. **82**, 3988 (1999).

[25] B. C. Collings, S. T. Cundiff, N. N. Akhmediev, J. M. Soto-Crespo, K. Bergman, and W. H. Knox, J. Opt. Soc. Am. B **17**, 354 (2000).

[26] C. Lecaplain, Ph. Grelu, J. M. Soto-Crespo, and N. Akhmediev, J. Opt. **15**, 064005 (2013).

[27] C. Lecaplain, Ph. Grelu, J. M. Soto-Crespo, and N. Akhmediev, Phys. Rev. Lett. **108**, 233901 (2012).

[28] V. Zharnitsky, I. Mitkov, and N. Grønbech-Jensen, Phys. Rev. E **58**, R52 (1998).

[29] A. P. Itin, Phys. Rev. E **63**, 028601 (2001).

[30] F. Kh. Abdullaev, E. N. Tsoy, B. A. Malomed, and R. A. Kraenkel, Phys. Rev. A **68**, 053606 (2003).

[31] J. Garnier, F. Kh. Abdullaev, and M. Salerno, Phys. Rev. E **75**, 016615 (2007).